Title

The gray matter structural connectome and its relationship to alcohol relapse: Reconnecting for recovery

Journal

Addiction Biology, 26(1)

ISSN

1355-6215

Authors

Mueller, Susanne G
Meyerhoff, Dieter J

Publication Date

2021

DOI

10.1111/adb.12860

Peer reviewed

Addiction Biology

SSA SOCIETY FOR THE STUDY OF ADDICTION

The Gray Matter Structural Connectome and its Relationship to Alcohol Relapse – Reconnecting for Recovery

Journal:	*Addiction Biology*
Manuscript ID	AB-07-2019-0176.R1
Wiley - Manuscript type:	Original Article
Date Submitted by the Author:	n/a
Complete List of Authors:	Mueller, Susanne; University of California San Francisco, Radiology and Biomedical Imaging; Center for Imaging of Neurodegenerative Diseases, VAMC Meyerhoff, Dieter; UCSF, Radiology
Keywords:	abstinence, alcohol use disorder, brain reward system
Abstract:	Gray matter (GM) atrophy associated with alcohol use disorders (AUD) affects predominantly the frontal lobes. Less is known how frontal lobe GM loss affects GM loss in other regions and how it influences drinking behavior or relapse after treatment. The Profile Similarity Index (PSI) combined with graph analysis allows to assess how GM loss in one region affects GM loss in regions connected to it, i.e. GM connectivity. The PSI was used to describe the pattern of GM connectivity in 21 Light Drinker (LD) and in 54 individuals with AUD (ALC) early in abstinence. Effects of abstinence and relapse were determined in a subgroup of 36 participants after 3 months Compared to LD, GM losses within the extended brain reward system (eBRS) at 1 month abstinence were similar between abstainers (ABST) and relapsers (REL), but REL had also GM losses outside the eBRS. Lower GM connectivities in ventro-striatal/hypothalamic and dorsolateral prefrontal regions and thalami were present in both ABST and REL. Between-networks connectivity loss of the eBRS in ABST was confined to prefrontal regions. About 3 months later, the GM volume and connectivity losses had resolved in ABST and insula connectivity was increased compared to LD. GM losses and GM connectivity losses in REL were unchanged. Overall, prolonged abstinence was associated with a normalization of within-eBRS connectivity and a reconnection of eBRS structures with other networks. The re-formation of structural connectivities within and across networks appears critical for cognitive-behavioral functioning related to the capacity to maintain abstinence after outpatient treatment.

The Gray Matter Structural Connectome and its Relationship to Alcohol Relapse – Reconnecting for Recovery

Susanne G. Mueller[1], Dieter J. Meyerhoff [1]

1. Center for Imaging of Neurodegenerative Diseases, Dept. of Radiology and Biomedical Imaging, University of California, San Francisco, CA. USA,

Corresponding author:
Susanne Mueller M.D.
Center for Imaging of Neurodegenerative Diseases
VAMC San Francisco
4150 Clement Street
San Francisco, CA, 94121
USA
e-mail: susanne.mueller@ucsf.edu
phone: 415 221 4810 ext 22538
FAX: 415 668 2864

Abstract

Gray matter (GM) atrophy associated with alcohol use disorders (AUD) affects predominantly the frontal lobes. Less is known how frontal lobe GM loss affects GM loss in other regions and how it influences drinking behavior or relapse after treatment. The Profile Similarity Index (PSI) combined with graph analysis allows **to assess how GM loss in one region affects GM loss in regions connected to it, i.e. GM connectivity**. **The PSI was used to describe the pattern of GM connectivity in 21 Light Drinker (LD) and in 54 individuals with AUD (ALC) early in abstinence.** Effects of abstinence and relapse were determined in a subgroup of 36 **participants** after 3 months **Compared to LD**, GM losses within **the extended brain reward system (eBRS)** at 1 month abstinence were similar between abstainers (ABST) and relapsers (REL), but REL had also GM losses outside the eBRS. Lower GM connectivities in ventro-striatal/hypothalamic and dorsolateral prefrontal regions and thalami were present in both ABST and REL. Between-networks connectivity loss of the eBRS in ABST was confined to prefrontal regions. About 3 months later, the GM volume and connectivity losses had resolved in ABST and insula connectivity was increased **compared to LD**. GM losses and GM connectivity losses in REL were unchanged. Overall, prolonged abstinence was associated with a normalization of within-eBRS connectivity and a reconnection of eBRS structures with other networks. The re-formation of structural connectivities within and across networks appears critical for cognitive-behavioral functioning related to the capacity to maintain abstinence after outpatient treatment.

Key words: abstinence, alcohol use disorder, brain reward system, relapse, gray matter connectivity, gray matter volume

Introduction

Cerebral atrophy is commonly observed on magnetic resonance imaging (MRI) of cortico-striatal-limbic structures from treatment-seeking **individuals with alcohol use disorder (ALC),** and it has been related to cognitive deficits and alcohol use behavior (for review see e.g. [1-3]). Quantitative MRI studies demonstrated a preference for gray matter (GM) atrophy and compromised white matter microstructural integrity in an extended brain reward system (eBRS) that encompasses orbitofrontal and dorsolateral prefrontal cortices, insula, anterior cingulate, striatum, thalami, hippocampi and amygdala [4-8]. Among ALC early in treatment, subsequent relapsers have greater brain structural and functional abnormalities than future abstainers, specifically in (prefrontal) top-down regions that, when intact, exert effective control over craving, stress-response and urge to drink during recovery [9-11].

But even relative focal pathologies in limbic regions or prefrontal cortex, for example, can affect neighboring and remote brain structures due to the loss of afferent and efferent projections between them. The pattern of GM volume losses resulting from these distributed effects can provide biologically valuable information regarding severity and localization of the primary morphological abnormalities and their behavioral downstream effects. Such regional patterns may potentially be more informative for understanding the neural alterations that relate to **alcohol use disorder (AUD)** or relapse after treatment than structural alterations of a few select brain nuclei/regions in isolation. Thus, different data analysis approaches have been developed to describe these patterns across neural networks. The most common approach has been to calculate large-scale GM volume or thickness covariance networks that are often characterized using graph analysis [12, 13]. One of the major limitations of such an approach is that the networks must be calculated at the population level, which prevents drawing conclusions on the single subject level and makes the inherent – though not necessarily true - assumption that all individuals

included in the analysis have similar patterns of morphological alterations. To overcome this limitation, several approaches have been proposed that use similarity measures to compare GM volumes/thickness of different brain regions directly within the individual brain [14-16]. One of them is the so-called profile similarity index (PSI) [16-18].The PSI assumes that an individual's GM volume loss in one region leads to a GM loss of similar severity in the individual's brain regions, which share strong direct afferent and efferent connections with it, due to the loss of these connections, whereas regional GM volumes without such connections are spared from volume loss and therefore "less similar".

In this study, we used the PSI to assess the impact of GM atrophy (or 'volume loss') on GM connectivity from ALC at 1 month of abstinence and from a subgroup of these individuals imaged about 3 months later after they either had remained abstinent (ABST) or relapsed to alcohol consumption (REL). As relapse is common among ALC within the first 6 months of treatment and related to brain dysfunction associated with chronic heavy drinking, we sought to investigate how abstinence and relapse are related to GM connectivity. Given our previous findings on the important role of the **extended brain reward system (eBRS**) in ALC and addiction in general [4, 5], we were particularly interested in the effects of abstinence and relapse on GM structural connectivity across eBRS structures (here termed 'within-eBRS' connectivity) and on the connectivity between eBRS and non-eBRS structures (termed 'between-networks' connectivity). We expected that ALC able to abstain from drinking for several months would not only have more GM early in abstinence but would also have a better preserved within-eBRS connectivity and a better integration of the eBRS with the rest of the brain than ALC who would relapse within a similar time interval. Furthermore, given the brain's plasticity following cessation of chronic drinking (for review see [19]) we expected that GM losses and connectivity abnormalities in early abstinence would (at least partially) resolve with prolonged abstinence.

Materials and Methods

Participants

We analyzed structural imaging data obtained from 54 ALC (mean age: 41.9 ± 10.0 years, min/max: 28-63) within 4 weeks of abstinence (timepoint 1 (TP1)), who had been recruited from the San Francisco Veterans Administration Medical Center Substance Abuse Day Hospital or the Kaiser Permanente Chemical Dependence Recovery outpatient treatment clinics, and 21 social or light drinkers (LD) (mean age: 46.2 ± 11.0 years, min/max: 26-65) recruited from the local community. 36 ALC (abstinent or relapsed) returned to undergo the same research procedures **approximately** 3 months later (TP2). LD were studied once and the data compared to ALC at both timepoints For basic group demographics see **Table 1.**

All participants were administered the screening section of the Structured Clinical Interview for DSM-IV or DSM5 Axis I disorder at baseline. **All 54 ALC were treatment-seeking with current moderate or severe AUD, 8 also had current moderate or severe cocaine use disorder**. **Of the 46 individuals with current AUD only, 6 also endorsed other current mild or moderate substance abuse by DSM-IV (mostly cocaine) and 3 currently used marijuana without reaching diagnostic criteria.** Exclusion criteria for both groups included histories of neurologic disease (e.g., epilepsy, traumatic brain injury, cerebrovascular disease), of general medical disease (e.g., untreated hypertension, diabetes, hypo/hyperthyroidism), and of psychiatric diseases (e.g., major depression, anxiety, trauma, and stress-related disorder). All participants also received a battery of interviews and standardized questionnaires that included the Beck Depression Inventory (BDI), Barratt Impulsiveness Scale (BIS), and standardized questionnaires assessing lifetime substance use (Lifetime Drinking and Smoking Histories). ALC had a history of consuming at least >150 standard alcoholic drinks per month (>80 for females) for >8 years (>6 years in females) before treatment, and LD had consumed fewer than 60 standard alcoholic drinks

in any month over lifetime (1 standard alcoholic drink contains 13.6 g of ethanol). Alcohol consumption between TPs was assessed at TP2 with an in-person Time Line Follow-Back interview [20]. The ALC were designated as abstainers (ABST) if they self-reported no alcohol consumption, if there were no reports of alcohol consumption in available medical records and when available laboratory indicators of alcohol consumption (e.g., γ-glutamyltransferase) were within normal limits at TP2. Participants were designated as Relapsers (REL) if they self-reported at TP2 any alcohol consumption after TP1 or had medical records of any alcohol consumption or relapse after TP1 procedures. The committees of human research at the University of California, San Francisco (UCSF) and the VA Medical Center had approved the study. Informed consent had been obtained from each participant prior to any research procedures in accordance with the Declaration of Helsinki.

Magnetic Resonance Imaging and image analysis

Image acquisition:

All MR data were acquired on a 3T Skyra system (Siemens, Erlangen, Germany) equipped with a 20 channel receive coil. The imaging protocol included different types of structural imaging, resting state fMRI and spectroscopy. Of these, only the T1-weighted whole brain gradient echo MRI (MPRAGE, TR/TE/TI = 2300/2.98/1000 ms, 1.0 x 1.0 x 1.0 mm^3 resolution, acquisition time = 5.30 minutes) was used for this report.

Image segmentation and parcellation:

The T1-weighted images underwent tissue segmentation with the new segment algorithm as implemented in SPM12 (https://www.fil.ion.ucl.ac.uk/spm). The resulting GM maps were warped onto a symmetrical GM template using DARTEL as implemented in SPM12. The Jacobian determinants from the warping step were calculated and used for spatial normalization and

modulation of the GM maps to the MNI space. The resulting spatially normalized GM maps underwent smoothing with a 4 mm FWHM Gaussian kernel and **correction for intracranial vault (ICV)** size (using the ICV volume calculated by adding up the gray, white and CSF maps in native space), after which age-corrected z-score maps [21] were calculated using the ranges observed in the ICV corrected, spatially normalized and rescaled GM maps of the TP1 images from the 21 LD plus 32 healthy reference subjects (mean age: 35.4 ± 12.9 years, min/max: 20-65) who had been studied with the same sequence on the same magnet. The AICHA parcellation [22] was used to extract the mean age corrected z-scores from 380 cortical and subcortical GM regions-of-interest (ROIs) (see **Figure 1**). As in previous reports by us [4, 5] **and others** [8], the eBRS region was composed of orbitofrontal, dorsolateral and anterior cingulate cortices, insula, striatum, thalami, hippocampi and amygdala.

Profile similarity index and graph theoretical approaches:

To investigate how the mean age-corrected GM z-score in one region related to that of the other 379 GM ROIs in the same participant, the PSI was calculated for each participant at each TP. The rawPSI between ROI x and ROI y is defined as follows:

$$\text{rawPSI} = (\text{ROI A} - \text{mean}_{\text{ROI}}) / \text{abs}((\text{ROI x} - \text{mean}_{\text{ROI}}) - (\text{ROI y} - \text{mean}_{\text{ROI}})),$$

where ROI is the mean of age-corrected GM z-score from voxels within the region-of-interest; ROI A is either ROI x or ROI y whichever is larger, mean_{ROI} is the mean of age corrected GM volume z-scores covered by all 380 AICHA regions. For participants with two TPs, the mean_{ROI} at TP1 was used to calculate the PSI at both TPs.

The rawPSI was calculated for each and every combination between two ROIs resulting in a 380x380 rawPSI matrix of ROIs for each individual's GM map at each TP. The rawPSI values that exceeded the 95th percentile of all PSI values in the map were replaced by the PSI value at

the 95th percentile in order to remove outliers caused by a difference of 0 or very small differences between ROI pairs. The rawPSI map was then converted into a final PSI map by multiplying it with a normalization term n defined as n = 1/(max rawPSI in map – min rawPSI in map). A negative PSI indicates a GM decrease in this ROI relative to this subject's mean whole brain GM; a positive PSI indicated a GM increase in this ROI relative to this subject's mean whole brain GM. It is assumed that the PSI map of an individual LD is determined by this person's individual anatomical features and, thus, that the PSI maps of the LD group captures the **most** common anatomical brain variants. A pathological process causing GM volume loss within the whole brain or a predefined subset of brain regions will introduce additional ROIs with relative GM decrease or increase and these will change the appearance of the resulting PSI map compared to a map from the LD group.

Graph theory was then used to summarize the pattern of relative GM decrease/increase captured by each participant's PSI map. The routines provided by the Brain Connectivity Toolbox (https://sites.google.com/site/bctnet) and in particular the weight conserving measure "strength", was used for this purpose [23]. Weight conserving measures have the advantage that they can be applied to fully connected networks, i.e., it is not necessary to define an arbitrary threshold to generate the type of sparse network required by the more commonly used non-weighted equivalent degree. Strength is defined as the sum of weights of links connected to a ROI. A ROI has a high strength when it experiences a similar degree of relative GM decrease as **many** other ROIs and a low strength when there are only few other ROIs with similar relative GM change. A brain with GM loss due to a more-or-less focal pathological process will have a different strength profile than a healthy brain. **If it is assumed that a similar degree of GM volume loss between two regions reflects a similar loss of axonal projections and/or of synapses connecting neurons, then GM loss equals GM connectivity loss and a high strength (referring here to GM loss) represents a more pronounced connectivity loss.**

Higher strength relative to another group will therefore be referred to as 'lower GM connectivity', lower strength as normalization or 'greater GM connectivity'. As stated in our *a priori* hypothesis, the impact of volume loss on within-eBRS structural connectivity and between-networks structural connectivity was of particular interest. **Figure 1** describes the major processing steps from T1-weighted MRI via image segmentation, PSI maps and graph analyses to within-eBRS and between-networks connectivity maps.

Figure 1 about here

Statistical Analysis

Fisher's Exact tests and t-tests were used to assess group differences of demographic and clinical measures shown in Table 1. Kruskal-Wallis tests were used to test for GM volume **differences** (expressed as age corrected z-scores) and GM connectivity differences (expressed as negative strength differences) at the ROI level between groups at different TP. False discovery rate (FDR**, q = 0.05**) was used to correct for multiple comparisons. However, as we set out to test specific *a priori* hypotheses, we also report FDR-uncorrected results ($p<0.05$) **for group comparisons where the effect size (epsilon square) was at least 'moderate', i.e. >0.04**[24]**. We do this for better illustration of** the pattern of GM loss and connectivity abnormalities **and in appreciation of the fact that such results may be meaningful even if they do not pass strict FDR-correction.**

Results

Demographics and Clinical Measures

The treatment-seekers were first studied at an average of 19 ± 9 days of abstinence from alcohol (TP1). Compared to LD, ALC scored higher on the BDI and BIS and – by design - on measures of lifetime alcohol use history **(see Table 1)**. Of the 36 ALC who returned for the TP2 study procedures, 24 were still abstinent (ABST) at TP2 (91.4 ± 17.7 days after TP1**, range: 63-121 days**) and 12 had relapsed (REL) at TP2 (104.9 ± 16.4 days after TP1, **range: 80 -132 days, p = 0.04**). ABST and REL did not differ on age, education, or our basic pre-treatment drinking and behavioral measures. At TP1, the basic characteristics of the patients with TP2 procedures were not different from those without TP2 procedures. On average, REL had consumed alcohol on 15 ± 13 days between TP1 and TP2 (range 1-36), with 99 ± 87 standard alcoholic drinks during relapse (range 4-261) and 8 ± 5 drinks per drinking day (range 3-20).

Table 1 about here

Gray matter volume

Compared to LD, ALC at TP1 (ABST and REL combined) had significant GM loss in bilateral dorsolateral frontal, supramarginal, right paracentral, temporo-polar and opercular regions, in septum/nucleus accumbens regions and in the right medial thalamus ($p<0.05$, FDR-corrected). Relaxing the significance criterium ($p<0.05$, no FDR correction) revealed volume loss also in bilateral medial and lateral prefrontal regions, bilateral insular, bilateral thalamic and midline regions.

Figure 2 contrasts GM volume loss in the combined ALC subgroups vs. LD and in ABST vs. REL at both TP1 and TP2. In short, REL had significantly more widespread GM losses than ABST, extending beyond the eBRS at both TPs, and particularly so at TP2 (bottom right), when brain

volumes in ABST were comparable to those in LD (top right). Specifically, both ABST and REL at TP1 displayed GM losses within eBRS structures at TP1, with more widespread eBRS GM losses in REL vs. LD than in ABS vs. LD. However, in direct comparisons of the ALC subgroups at TP1 (FDR), REL had significantly less GM than ABST in the right supramarginal cortex only; however, at TP2, their volume losses were more widespread and significant, including in a large region in the left parietal cortex and a small region in the right thalamus.

Figure 2 about here

Gray matter connectivity

TP1 cross-sectional results: LD versus ALC at baseline

Within-eBRS connectivity was lower in the right septum, right medial thalamus and the left dorsolateral frontal region of ALC at TP1 compared to LD ($p<0.05$, FDR). Relaxing the significance criterium ($p<0.05$, no FDR) identified additional regions with lower connectivity in the right subgenual region, the right anterior cingulate, right dorsolateral frontal region and the bilateral septum.

Between-networks connectivity in ALC at TP1 vs. LD was lower with the left supramarginal gyrus ($p<0.05$, FDR). At the lower significance threshold, we identified additional regions of lower between-networks connectivity with the bilateral supramarginal gyrus; the left paracentral lobule had higher between-networks connectivity in ALC vs. LD.

Within-eBRS connectivity across both TPs

Figure 3 displays the within-eBRS connectivity strengths maps in ABST and REL at both TPs and in LD at TP1 only (upper panel), while **Figure 4** shows the corresponding statistical maps for the group comparisons. At TP1, within-eBRS connectivity in ABST was relatively lowest in subcortical structures, i.e., thalamus, putamen, pallidum, septal structures and parts of the insula. The FDR-corrected statistical maps in **Figure 4** showed that compared to LD, within-eBRS connectivity in ABST was significantly lower in the right septum and the left dorsolateral prefrontal region. Without FDR-correction, additional regions of lower connectivity in ABST were revealed in left septum, left insula/operculum and bilateral medial thalamus and dorsolateral prefrontal regions (**Figure 4**). In REL at TP1, the within-eBRS connectivity strength map showed regions of relatively low connectivity in prefrontal brain (**Figure 3**). Statistically, the within-eBRS connectivities in the right dorsolateral prefrontal and subgenual cingulate regions were lower ($p<0.05$, FDR) in REL than LD (**Figure 4**). Additional regions in the bilateral medial thalamus, left anterior cingulate and left dorsolateral prefrontal brain were identified without FDR-correction. A direct comparison between ABST and REL confirmed the similarity of the pattern of abnormal within-eBRS connectivity in the two subgroups at TP1 (**Figure 3**); the only group difference was a lower left insula/operculum connectivity in REL vs. ABST ($p<0.05$, no FDR) (**Figure 4**, bottom left).

At TP2, about 3 months after TP1, the within-eBRS connectivity map in ABST showed a pattern very similar to that in LD (**Figure 3** top row), with the within-eBRS connectivity in ABST being no longer different from that in LD after FDR correction (**Figure 4**). Without FDR-correction, ABST at TP2 showed a higher GM connectivity in the bilateral insula/operculum region than LD. In contrast, the pattern and degree of within-eBRS connectivity strength in REL at TP2 compared to LD appeared more abnormal than at TP1 (**Figure 3** top), which can also be appreciated in the statistical maps (**Figure 4**). Relaxing the significance criterium identified additional regions of lower within-eBRS connectivity in the right hippocampus and bilateral insula/opercular regions of

REL. Furthermore and as hypothesized, the within-eBRS connectivity differences between ABST and REL were more pronounced at TP2: GM connectivity was lower in left medial prefrontal cortex and bilateral insula/operculum regions of REL compared to ABST ($p<0.05$, FDR), with more regions of lower within-eBRS connectivity becoming visible in the right dorsolateral prefrontal regions, bilateral medial thalamus, as well as bilateral septum and anterior cingulate at the lower significance threshold (**Figure 4**).

Figures 3 and **4** about here

Between-networks connectivity across both TPs

The lower section of **Figure 3** shows the between-networks connectivity strength maps in each subgroup at both TPs, while **Figure 5** shows the corresponding statistical maps for our main group comparisons. The between-networks connectivity strength maps in ABST at TP1 were very similar in appearance to those from LD, as also confirmed by the statistical analysis (FDR). **Without FDR correction**, lower connectivity in ABST became apparent in the left and right anterior cingulate and right inferior orbital frontal regions. In contrast, the between-networks connectivity maps from REL showed regions with altered connectivity of the lateral parieto-occipital region (**Figure 3**). The statistical analysis showed a region of lower between-networks connectivity with the right supramarginal gyrus in REL at TP1 compared to LD ($p<0.05$, FDR) (**Figure 5**). At the lower significance threshold, we identified additional regions with lower between-networks connectivity in the supramarginal gyrus and the mid-cingulate bilaterally and in the left inferior parietal lobule, right medial prefrontal region and left mid and inferior temporal gyrus. This comparison of REL vs. LD also showed regions with higher between-networks

connectivity in the right paracentral lobule, the right supplementary motor cortex and right precuneus and in the left paracentral lobule and precentral gyrus.

The direct comparison between the two ALC subgroups at TP1 showed a region of higher between-networks connectivity with the right paracentral lobule of REL vs. ABST ($p<0.05$, FDR) (**Figure 5**). **At $p<0.05$ uncorrected**, REL showed regions of lower GM connectivities within the right mid-cingulate gyrus, the right supramarginal gyrus, and the inferior parietal lobule bilaterally as well as higher connectivity of the paracentral lobule bilaterally.

At TP2, between-networks connectivity strengths maps from ABST were very similar to those of LD (**Figure 3**), as confirmed in the statistical analysis ($p<0.05$, FDR) (**Figure 5**). This was reminiscent of the GM volume analysis. **Without FDR-correction**, between-networks connectivity was higher in several ROIs of the bilateral medial and lateral parietal and occipital lobe and frontal superior gyrus of ABST vs. LD. In contrast, the pattern of altered between-networks connectivity in REL compared to LD was more pronounced at TP2 than at TP1 (**Figure 3**), and the corresponding statistical analyses confirmed that observation (**Figure 5**).

The direct comparison between ABST and REL at TP2 identified lower eBRS between-network connectivity with the supramarginal gyrus and operculum, bilaterally, left inferior parietal gyrus and insula and right lateral occipital lobe ($p<0.05$, FDR) of REL (**Figure 5**). Lower significance levels identified even more widespread ROIs with lower connectivity in REL vs. ABST, specifically of the medial and lateral frontal, parietal and occipital lobes bilaterally, including precuneus, posterior cingulate and superior and inferior temporal gyri.

Figure 5 about here

Discussion

This study characterized GM connectivity abnormalities caused by GM volume loss within eBRS structures and between eBRS and other brain structures as a function of alcohol relapse status. The profile similarity index (PSI) described the degree to which volumes of cortical and subcortical GM change 'in tandem with' ('similar to') GM volumes of other brain regions that are structurally connected via direct afferent and efferent connections. The major findings were: 1.) The pattern of GM volume losses in ALC after **about 3**weeks of abstinence (at TP1) was largely consistent with the spatial pattern described in other structural imaging studies [7]. Both ABST and REL displayed similar magnitudes of GM losses within eBRS structures, but only REL had GM losses also outside the eBRS. About 3 months later (at TP2), the GM volume losses had resolved in ABST only. 2.) GM volume losses negatively affected within-eBRS connectivity: Lower GM connectivities in ventro-striatal/hypothalamic and dorsolateral prefrontal regions and midline thalamus were present in ALC and in both subgroups after **about 3** weeks of abstinence. At TP2, after 3 additional months of abstinence, the earlier within-eBRS GM connectivity loss had either completely resolved, or the connectivity was even stronger in the insula compared to that in LD. By contrast, the pattern of within-eBRS connectivity loss in REL was largely comparable at both TPs, but it differed significantly from that in ABST at TP2. 3.) In accordance with widespread GM volume loss, REL at both TPs displayed GM connectivity losses of the eBRS with mostly temporal and parietal (non-eBRS) regions. On the other hand, the between-networks connectivity loss of the eBRS in ABST at TP1 was only confined to links with prefrontal regions. Continued abstinence resulted in a normalization of the within-eBRS connectivity at TP2 and a better integration (i.e., reconnection) of eBRS structures with regions of other brain networks. Together with previous research, our results suggest that in addition to the structural and metabolic integrity of eBRS structures [9, 25], the intactness of and strength of connectivities to non-eBRS regions play a critical role in the capability of ALC to sustain abstinence after treatment for **AUD**.

Gray matter volume

After **about 3** weeks of abstinence, ALC showed less GM (relative to LD) in bilateral dorsolateral and medial prefrontal and lateral temporal regions, in the insula, medial thalamus and ventral striatum/hypothalamus bilaterally, consistent with volume loss described elsewhere [7, 9]. **In contrast to another recently published study, we detected no GM loss in the cuneus/precuneus** [26]. This early in abstinence, GM loss in participants able to maintain abstinence beyond 3 months (ABST) was mostly confined to the eBRS and neighboring prefrontal regions. Those participants who were unable to maintain abstinence over 3 months (REL) had visually more pronounced GM losses at TP1 in the eBRS regions and in regions that extended further into the parietal, occipital and temporal lobes. While the regional eBRS volume differences between ABST and REL were not statistically significant after FDR corrections, volumes in non-eBRS regions differed at lower significance levels. About 3 months after TP1, GM differences were no longer significant between ABST and LD, but significant GM loss was still present in REL, who had resumed some degree of drinking after TP1.

Gray matter connectivity

After about 3 weeks of abstinence, the entire group of ALC and the subgroups of ABST and REL showed within-eBRS GM connectivity losses in the bilateral ventral striatum/hypothalamus, dorsolateral prefrontal regions, and in the midline thalamus nuclei when compared to LD. Although REL also displayed GM connectivity losses in the medial prefrontal cortex, i.e., in the anterior and subgenual cingulate that was not present in ABST, the groups were not different from each other in direct comparisons at TP1. Taken together, in both subgroups eBRS GM loss resulted in compromised GM connectivity in eBRS regions that are also involved in the modulation of emotional stress and anxiety, potentially facilitating stress-associated alcohol craving and

alcohol seeking behavior [27-31], and in regions associated with executive control and attention. Volume loss and associated dysfunctions in these brain regions can contribute to maladaptive substance use behavior [32].

ALC who had relapsed between TP1 and TP2 (REL) showed essentially the same pattern of within-eBRS GM connectivity loss at both TPs, whereas the initial within-eBRS connectivity abnormalities in ABST had completely resolved at TP2. In contrast to REL, ABST also showed greater connectivity of anterior and posterior insula with other eBRS structures. The insula is involved in processing of interoceptive signals and is thought to play an important role in the conscious experience of various types of bodily information (such as from the effects of alcohol on the body) and in the conscious recalling of this experience when exposed to alcohol-associated cues [33-35]. The stronger connectivity of the insula within the eBRS network of ABST can be interpreted as evidence for a better integration of the insula with eBRS structures that also belong to the salience network [36], i.e., anterior cingulate, medial thalamus, amygdala, and with eBRS structures belonging to the executive control network [37], i.e., dorsolateral prefrontal regions. These reconnections or improved interactions between these critical networks could explain why ABST are able to deal better with alcohol cravings or other life stressors than REL and therefore manage to maintain their abstinence more effectively.

Regarding the degree to which GM losses extended beyond the eBRS in each group, between-networks GM connectivity losses in ABST were restricted to small prefrontal regions proximal to the eBRS, whereas REL showed more distal between-networks connectivity losses to supramarginal gyri, inferior parietal lobules, the mid/posterior cingulate regions bilaterally and to the left middle and inferior temporal gyri. Studies using task-based functional fMRI and structural MRI showed that parietal and middle temporal together with dorsolateral prefrontal regions play a crucial role in delayed discounting and in suppressing impulsive decisions [38-41], critical concepts

in resisting the urge to drink. In addition to its shrinkage [10, 11], altered functional connectivity of the cingulate in response to alcohol and stress cues has been shown to be associated with greater alcohol relapse risk [42]. These functional studies suggest that the compromised between-networks structural connectivity on top of the within-eBRS connectivity losses could have contributed to the REL's inability to abstain from alcohol after treatment.

Interestingly, between-networks connectivity strength was higher for sensorimotor regions in REL compared to LD. **Altered gm connectivity has to be interpreted in the behavioral context, i.e., increased gm connectivity does not always imply normal or better function/behavior and *vice versa*. In this study, greater connectivity links regions with normal GM volume (sensorimotor) to the eBRS that encompasses regions with both normal GM and GM loss. A GM connectivity increase in this context points to a connectivity reconfiguration in which connectivity loss to regions with GM loss is accompanied by increased connectivity to regions with normal GM. Such a reconfiguration is likely to be associated with behavioral consequences. An example how such behavioral consequences could manifest themselves in the sensorimotor area was recently described by Quoilin et al. [43], who observed an impaired neural inhibition in recently abstinent ALC compared to LD when motor event potentials were elicited immediately before voluntary movements; the impaired neural inhibition was more pronounced in those ALC who later relapsed.**

As observed for the within-eBRS network connectivity (and GM volume loss), the patterns of altered between-networks connectivity of REL were similar at both TPs. By contrast, although ABST at TP1 had significant GM loss/connectivity abnormalities only in the eBRS, the GM connectivities of the eBRS at TP2 to the bilateral precuneus, lateral parietal and occipital regions exceeded those in LD. This indicates effective recovery and normalization from eBRS GM losses observed early in abstinence, if not even a stronger integration of the eBRS regions (i.e.,

reconnection) with nodes of the default mode network (precuneus), the executive network (lateral parietal regions) and the visual network (occipital regions). Stronger distributed connectivities across neural networks therefore may reflect the greater resilience of ABST to alcohol relapse,

The main limitations of our analyses include our inability to effectively assess sex and smoking effects. Only about 1/3 of our study participants were female, resulting in rather small subgroups when stratified by relapse status. Previous research has demonstrated effects of smoking on cortical thickness in eBRS regions [4, 44, 45] and differential cortical volume recovery during abstinence [46]. While trying to understand if chronic smoking affects structural connectivities and potentially related substance use behavior (it does affect functional connectivities, e.g., [47] and frontal brain microstructure, e.g., [48]) has practical clinical value, the proportion of smokers and non-smokers was unbalanced across our ALC subgroups, though not different ($p = 0.11$, Fisher's exact test), preventing meaningful analyses. **Excluding the 8 individuals with comorbid substance use disorder in tertiary analyses did not change the main results of the study.** Finally, **the imaging data were processed cross-sectionally, i.e., each TP was analyzed separately instead of calculating longitudinal changes or intermediate images.**

In conclusion, whereas in previous work we and others related the shrinkage of select brain regions to alcohol relapse, here we identified regional patterns of GM volume and structural connectivity losses across the brain that relate to inability to maintain abstinence after treatment for AUD. Our findings suggest that it is not only the severity of the GM volume loss within eBRS structures *per se* (such as in the ventral striatum/hypothalamus and prefrontal cortex) or the connectivity losses within eBRS structures *per se* that determine risk for relapse. Rather, it is the degree to which brain GM regions, which are structurally connected to the eBRS and subserve self-control, handling stressors and suppressing craving, are structurally intact and able to re-

connect with the eBRS as the injured brain recovers after drinking cessation. This functionally relevant structural (re)connection of eBRS regions to proximal and distant cortical regions, which are inefficiently connected during chronic and excessive alcohol consumption, distinguishes successful abstainers from future relapsers in the months following outpatient treatment. As such, at more than one level of meaning, restoring severed connections is critical for successful recovery after treatment.

Acknowledgement: The work was supported by grant NIH R01 AA10788 (DJM) and R01 DA039903 (DJM).

Author contributions: DJM obtained funding for the research and was responsible for study design and data interpretation. SGM was responsible for data processing and analysis and was instrumental for data interpretation. SGM drafted the manuscript and both authors provided important intellectual input, critically reviewed content and approved the final version of the manuscript.

Table 1: Group demographics

TP 1	**LD**	**ALC**	
n	21	54	
Age	46.9 ± 11.2	42.0 ± 10.0	
Gender M/F	16/5	34/20	
Smoking Yes/No	8/13	19/35	
Years Education	15.7 ±1.9	14.9 ± 2.1	
BDI	3.9 ± 4.9	12.0 ± 7.1*	
BIS	57.9 ± 10.3	66.1 ± 11.2*	
Lifetime Average Drinks/Month	13.0 ± 11.5	178.3 ± 88.8*	
Months Heavy Drinking	0	165.6 ± 106.1*	
TP2		**ABST**	**REL**
n		24	12
Age		41.4 ± 11.1	41.4 ± 8.9
Gender M/F		16/8	8/4
Smoking Yes/No		9/15	1/11
Years Education		14.6 ± 2.4*	15.2 ± 2.2
BDI		11.8 ± 6.8*	13.3 ± 8.0*
BIS		67.5 ± 8.1*	64.2 ± 12.7*
Lifetime Average Drinks/Month		191.8 ± 114.6*	147.4 ± 46.6*
Months Heavy Drinking		162.0 ± 101.8*	143.8 ± 85.9*

* $p<0.05$ compared to LD

LD = Light Drinker; ALC = **individuals with alcohol use disorder**; ABST = abstainer at TP2; REL = relapsers at TP2; BDI = Beck Depression inventory score; BIS = Barratt Impulsiveness Scale score. 'Heavy Drinking' defined as drinking at >100 drinks/month in males and >80 drinks/month in females

Legends

Figure 1. **Processing steps for PSI and connectivity calculations**. A. Between-networks connectivity processing: The connectivity analysis is restricted to connections between within-eBRS ROIs (indicated in blue on axial brain image) with other brain ROIs (in orange) as indicated by yellow lines in the PSI mask, while PSI information between other brain ROIs is suppressed as indicated by blue lines in the PSI mask. B. Within-eBRS connectivity processing: The connectivity analysis is restricted to connections between ROIs of the eBRS (prefrontal cortices, insula, striatum, thalami, hippocampi and amygdala, indicated in blue on brain images).

Figure 2. **Regions with GM volume losses in ABST and REL at TP1 and TP2.** The top section contrasts ABST with LD, the middle section REL with LD, and the bottom section REL with ABST. The different colors signify different significance levels ($p<0.05$ with and without FDR correction).

Figure 3. **Within- and between-networks gray matter connectivity maps**. Gray matter connectivity Top row: Population within-eBRS connectivity strength maps in controls, ABST and REL at TP1 (left side) and TP2 (right side). Image left is patient left. Lower rows: Population between-networks connectivity strength maps in controls, ABST and REL at TP1 (left) and TP2 (right). Color bars: Brighter colors or higher numbers indicate ROIs with relatively greater connectivity losses (less connectivity).

Figure 4. Statistical maps of within-eBRS connectivity. Within-eBRS connectivity differences for different group comparisons at TP1 (left) and TP2 (right). The different colors signify different significance levels ($p<0.05$ with and without FDR correction). Image left is patient left. See text for details.

Figure 5. **Statistical maps of between-networks connectivity differences** at TP (left) and TP2 (right) for different group comparisons. eBRS regions are overlaid in dark gray.

The different colors signify different significance levels ($p<0.05$ with and without FDR correction).

Image left is patient left. See text for details.

References

1. Zahr NM, Pfefferbaum A, Sullivan EV. Perspectives on fronto-fugal circuitry from human imaging of alcohol use disorders. *Neuropharmacology* 2017; 122:189-200.

2. Schulte T, Oberlin BG, Kareken DA, Marinkovic K, Muller-Oehring EM, Meyerhoff DJ, et al. How acute and chronic alcohol consumption affects brain networks: insights from multimodal neuroimaging. *Alcohol ClinExpRes* 2012; 36(12):2017-2027.

3. Sullivan EV, Harris RA, Pfefferbaum A. Alcohol's effects on brain and behavior. *Alcohol Res Health* 2010; 33(1-2):127-143.

4. Durazzo TC, Mon A, Gazdzinski S, Meyerhoff DJ. Chronic cigarette smoking in alcohol dependence: associations with cortical thickness and N-acetylaspartate levels in the extended brain reward system. *Addict Biol* 2013; 18(2):379-391.

5. Kuceyeski A, Meyerhoff DJ, Durazzo TC, Raj A. Loss in connectivity among regions of the brain reward system in alcohol dependence. *Hum Brain Mapp* 2013; 34(12):3129-3142.

6. Volkow ND, Baler RD. Brain imaging biomarkers to predict relapse in alcohol addiction. *JAMA psychiatry* 2013; 70(7):661-663.

7. Yang X, Tian F, Zhang H, Zeng J, Chen T, Wang S, et al. Cortical and subcortical gray matter shrinkage in alcohol-use disorders: a voxel-based meta-analysis. *Neurosci Biobehav Rev* 2016; 66:92-103.

8. Makris N, Oscar-Berman M, Jaffin SK, Hodge SM, Kennedy DN, Caviness VS, et al. Decreased volume of the brain reward system in alcoholism. *Biol Psychiatry* 2008; 64(3):192-202.

9. Durazzo TC, Tosun D, Buckley S, Gazdzinski S, Mon A, Fryer SL, et al. Cortical thickness, surface area, and volume of the brain reward system in alcohol dependence: relationships to relapse and extended abstinence. *Alcohol ClinExpRes* 2011; 35(6):1187-1200.

10. Rando K, Hong KI, Bhagwagar Z, Li CS, Bergquist K, Guarnaccia J, et al. Association of frontal and posterior cortical gray matter volume with time to alcohol relapse: a prospective study. *Am J Psychiatry* 2011; 168(2):183-192.

11. Beck A, Wustenberg T, Genauck A, Wrase J, Schlagenhauf F, Smolka MN, et al. Effect of brain structure, brain function, and brain connectivity on relapse in alcohol-dependent patients. *Arch Gen Psychiatry* 2012; 69(8):842-852.

12. He Y, Evans A. Graph theoretical modeling of brain connectivity. *Curr Opin Neurol* 2010; 23(4):341-350.

13. Alexander-Bloch A, Raznahan A, Bullmore E, Giedd J. The convergence of maturational change and structural covariance in human cortical networks. *J Neurosci* 2013; 33(7):2889-2899.

14. Tijms BM, Series P, Willshaw DJ, Lawrie SM. Similarity-based extraction of individual networks from gray matter MRI scans. *Cereb Cortex* 2012; 22(7):1530-1541.

15. Mueller SG, Bateman LM, Laxer KD. Evidence for brainstem network disruption in temporal lobe epilepsy and sudden unexplained death in epilepsy. *NeuroImage Clinical* 2014; 5:208-216.

16. Mueller SG, Weiner MW. Amyloid Associated Intermittent Network Disruptions in Cognitively Intact Older Subjects: Structural Connectivity Matters. *Front Aging Neurosci* 2017; 9:418.

17. Mueller SG, Nei M, Bateman LM, Knowlton R, Laxer KD, Friedman D, et al. Brainstem network disruption: A pathway to sudden unexplained death in epilepsy? *Hum Brain Mapp* 2018; 39(12):4820-4830.

18. Mueller SG, Bateman LM, Nei M, Goldman AM, Laxer KD. Brainstem atrophy in focal epilepsy destabilizes brainstem-brain interactions: Preliminary findings. *NeuroImage Clinical* 2019; 23:101888.

19. Meyerhoff DJ, Durazzo TC. Modeling cognitive and neurobiological recovery in addiction. Chapter in "Cognition and Addiction: A researcher's guide from mechanisms towards interventions". 2019.

20. Sobell LC, Sobell MB, Riley DM, Schuller R, Pavan DS, Cancilla A, et al. The reliability of alcohol abusers' self-reports of drinking and life events that occurred in the distant past. *J Stud Alcohol* 1988; 49(3):225-232.

21. O'Brien PC, Dyck PJ. Procedures for setting normal values. *Neurology* 1995; 45(1):17-23.

22. Joliot M, Jobard G, Naveau M, Delcroix N, Petit L, Zago L, et al. AICHA: An atlas of intrinsic connectivity of homotopic areas. *J Neurosci Methods* 2015; 254:46-59.

23. Rubinov M, Sporns O. Weight-conserving characterization of complex functional brain networks. *Neuroimage* 2011; 56(4):2068-2079.

24. Rea LM, Parker RA. Designing and conducting survey research: A comprehensive guide. San Francisco: Jossery - Bass, 4th ed, 2014.

25. Durazzo TC, Pathak V, Gazdzinski S, Mon A, Meyerhoff DJ. Metabolite levels in the brain reward pathway discriminate those who remain abstinent from those who resume hazardous alcohol consumption after treatment for alcohol dependence. *Journal of Studies on Alcohol and Drugs* 2010; 71(2):278-289.

26. Wang J, Fan Y, Dong Y, Ma M, Dong Y, Niu Y, et al. Combining gray matter volume in the cuneus and the cuneus-prefrontal connectivity may predict early relapse in abstinent alcohol-dependent patients. *PLoS One* 2018; 13(5):e0196860.

27. Sinha R, Li CS. Imaging stress- and cue-induced drug and alcohol craving: association with relapse and clinical implications. *Drug Alcohol Rev* 2007; 26(1):25-31.

28. Seo D, Lacadie CM, Tuit K, Hong KI, Constable RT, Sinha R. Disrupted ventromedial prefrontal function, alcohol craving, and subsequent relapse risk. *JAMA Psychiatry* 2013; 70(7):727-739.

29. Seo D, Sinha R. The neurobiology of alcohol craving and relapse. *Handbook of Clinical Neurology* 2014; 125:355-368.

30. Pahng AR, McGinn MA, Paulsen RI, Edwards S. The Prefrontal Cortex as a Critical Gate of Negative Affect and Motivation in Alcohol Use Disorder. *Current Opinion in Behavioral Sciences* 2017; 13:139-143.

31. Forster SE, Dickey MW, Forman SD. Regional cerebral blood flow predictors of relapse and resilience in substance use recovery: A coordinate-based meta-analysis of human neuroimaging studies. *Drug Alcohol Depend* 2018; 185:93-105.

32. Tanabe J, Regner M, Sakai J, Martinez D, Gowin J. Neuroimaging reward, craving, learning, and cognitive control in substance use disorders: review and implications for treatment. *Br J Radiol* 2019:20180942.

33. Droutman V, Read SJ, Bechara A. Revisiting the role of the insula in addiction. *Trends Cogn Sci* 2015; 19(7):414-420.

34. Naqvi NH, Gaznick N, Tranel D, Bechara A. The insula: a critical neural substrate for craving and drug seeking under conflict and risk. *Ann N Y Acad Sci* 2014; 1316:53-70.

35. Sinha R. Disgust, insula, immune signaling, and addiction. *Biol Psychiatry* 2014; 75(2):90-91.

36. Seeley WW, Menon V, Schatzberg AF, Keller J, Glover GH, Kenna H, et al. Dissociable Intrinsic Connectivity Networks for Salience Processing and Executive Control. *The Journal of Neuroscience* 2007; 27(9):2349-2356.

37. Dosenbach NU, Fair DA, Miezin FM, Cohen AL, Wenger KK, Dosenbach RA, et al. Distinct brain networks for adaptive and stable task control in humans. *Proc Natl Acad Sci U S A* 2007; 104(26):11073-11078.

38. Amlung M, Sweet LH, Acker J, Brown CL, MacKillop J. Dissociable brain signatures of choice conflict and immediate reward preferences in alcohol use disorders. *Addict Biol* 2014; 19(4):743-753.

39. Owens MM, Gray JC, Amlung MT, Oshri A, Sweet LH, MacKillop J. Neuroanatomical foundations of delayed reward discounting decision making. *Neuroimage* 2017; 161:261-270.

40. McClure SM, Laibson DI, Loewenstein G, Cohen JD. Separate neural systems value immediate and delayed monetary rewards. *Science* 2004; 306(5695):503-507.

41. McClure SM, Ericson KM, Laibson DI, Loewenstein G, Cohen JD. Time discounting for primary rewards. *J Neurosci* 2007; 27(21):5796-5804.

42. Zakiniaeiz Y, Scheinost D, Seo D, Sinha R, Constable RT. Cingulate cortex functional connectivity predicts future relapse in alcohol dependent individuals. *NeuroImage Clinical* 2017; 13:181-187.

43. Quoilin C, Wilhelm E, Maurage P, de Timary P, Duque J. Deficient inhibition in alcohol-dependence: let's consider the role of the motor system! *Neuropsychopharmacology* 2018; 43(9):1851-1858.

44. Kuhn S, Schubert F, Gallinat J. Reduced thickness of medial orbitofrontal cortex in smokers. *Biol Psychiatry* 2010; 68(11):1061-1065.

45. Karama S, Ducharme S, Corley J, Chouinard-Decorte F, Starr JM, Wardlaw JM, et al. Cigarette smoking and thinning of the brain's cortex. *Mol Psychiatry* 2015; 20(6):778-785.

46. Zou X, Durazzo TC, Meyerhoff DJ. Regional Brain Volume Changes in Alcohol-dependent Individuals during Short-term and Long-term Abstinence. *Alcohol ClinExpRes* 2018.

47. Jasinska AJ, Zorick T, Brody AL, Stein EA. Dual role of nicotine in addiction and cognition: a review of neuroimaging studies in humans. *Neuropharmacology* 2014; 84:111-122.

48. Lin F, Wu G, Zhu L, Lei H. Heavy smokers show abnormal microstructural integrity in the anterior corpus callosum: a diffusion tensor imaging study with tract-based spatial statistics. *Drug Alcohol Depend* 2013; 129(1-2):82-87.

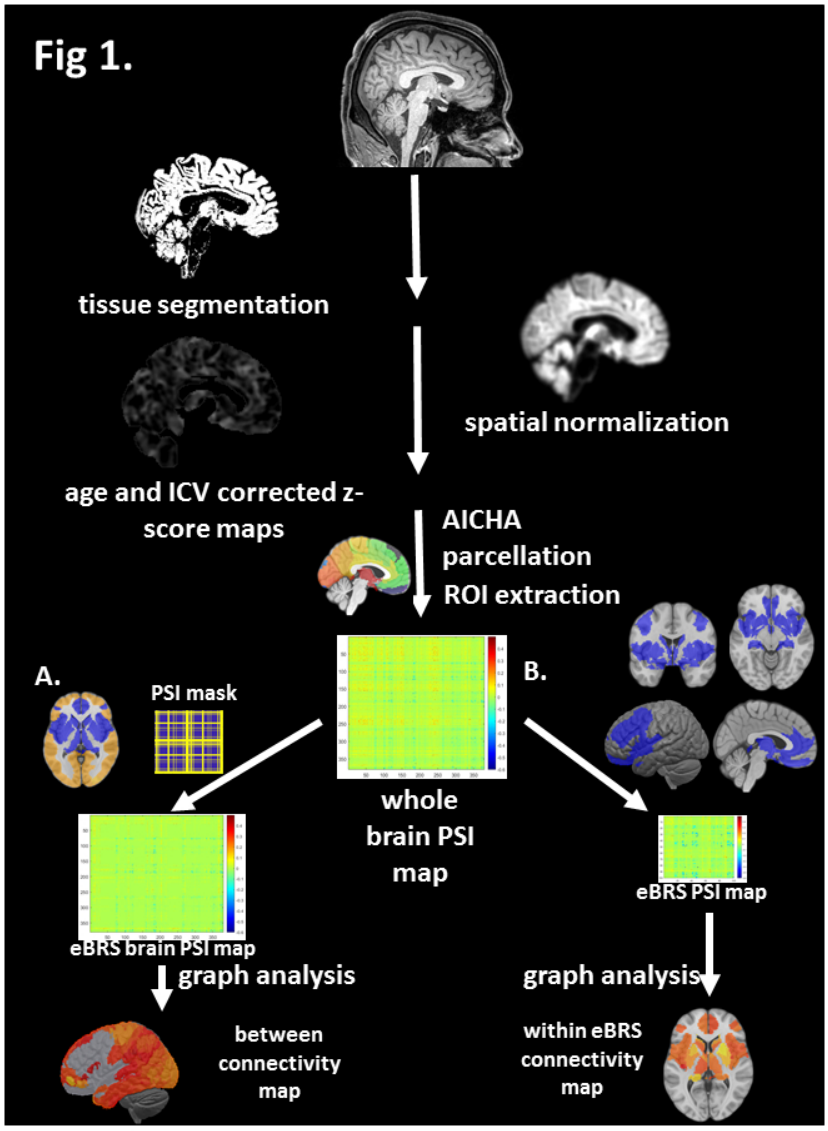

Figure 1. Processing steps for PSI and connectivity calculations. A. Between-networks connectivity processing: The connectivity analysis is restricted to connections between within-eBRS ROIs (indicated in blue on axial brain image) with other brain ROIs (in orange) as indicated by yellow lines in the PSI mask, while PSI information between other brain ROIs is suppressed as indicated by blue lines in the PSI mask. B. Within-eBRS connectivity processing: The connectivity analysis is restricted to connections between ROIs of the eBRS (prefrontal cortices, insula, striatum, thalami, hippocampi and amygdala, indicated in blue on brain images).

60x81mm (300 x 300 DPI)

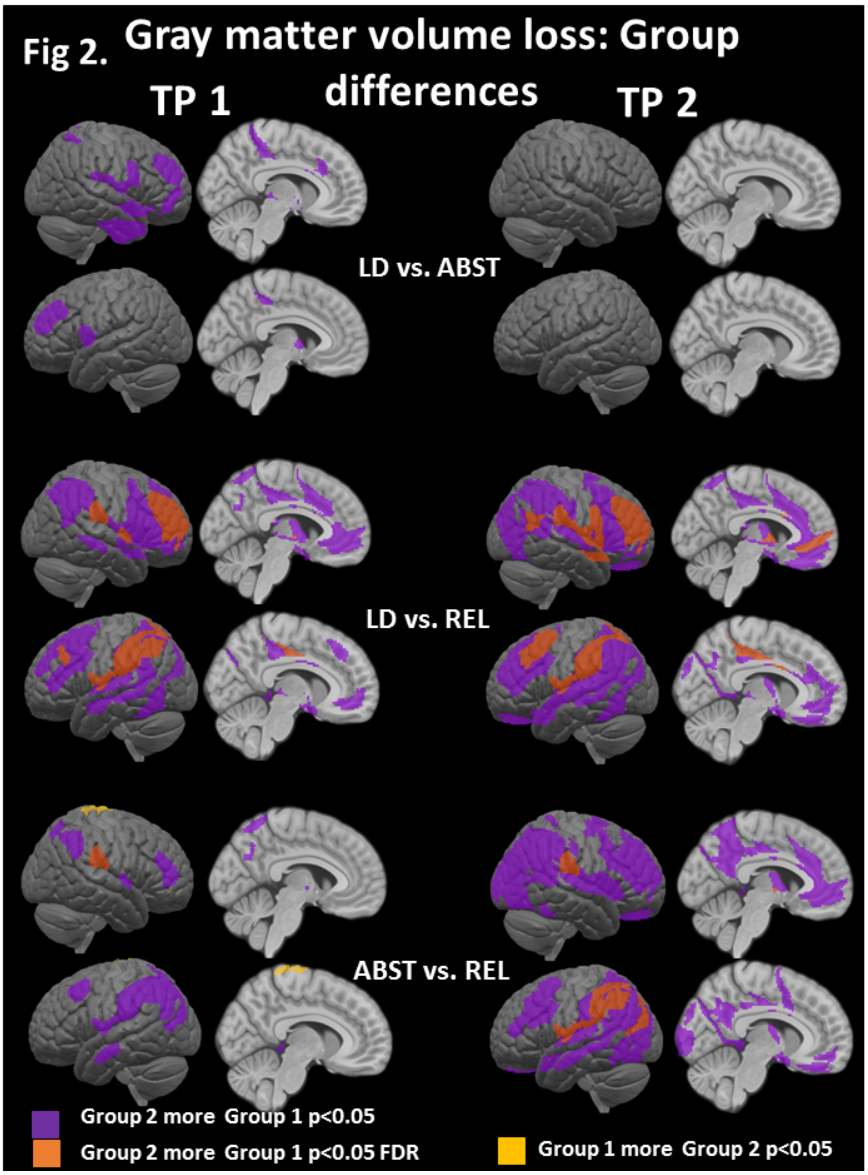

Figure 2. Regions with GM volume losses in ABST and REL at TP1 and TP2. The top section contrasts ABST with LD, the middle section REL with LD, and the bottom section REL with ABST. The different colors signify different significance levels ($p<0.05$ with and without FDR correction).

60x81mm (300 x 300 DPI)

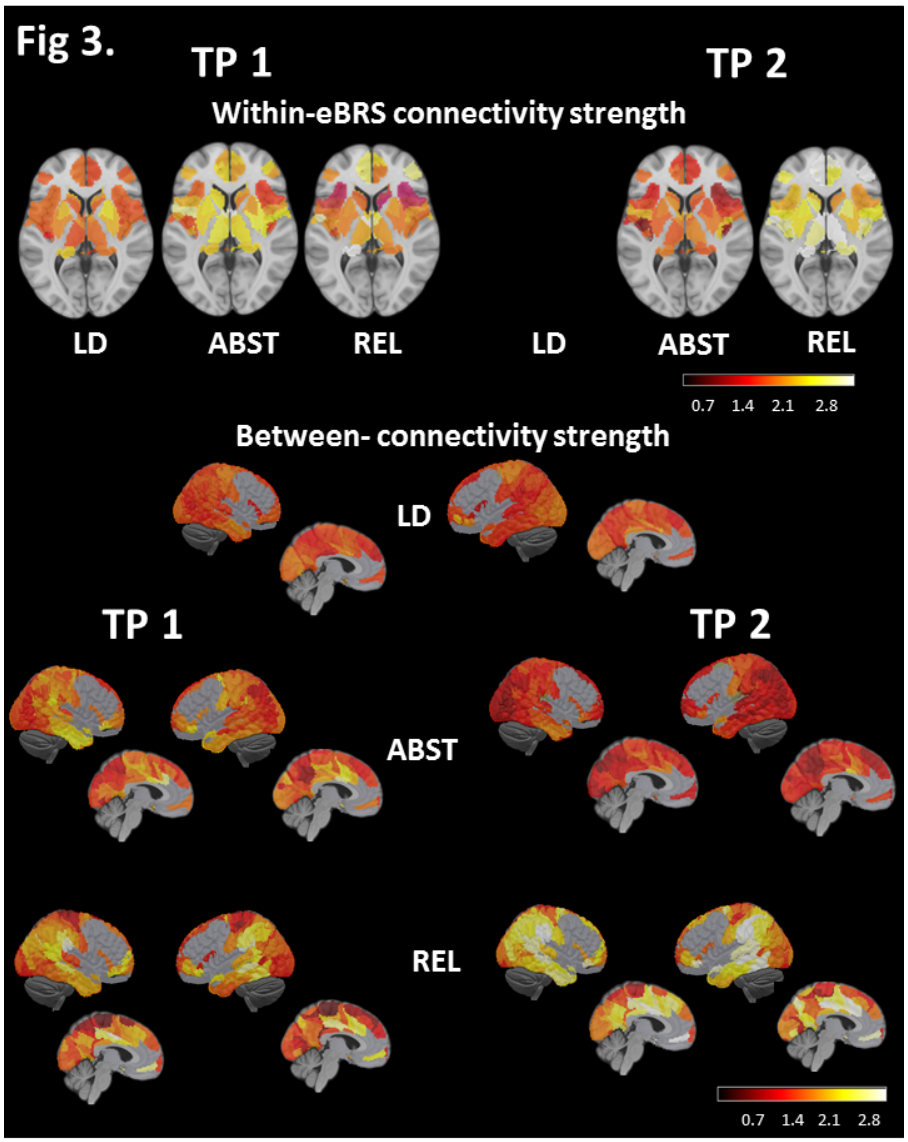

Figure 3. Within- and between-networks gray matter connectivity maps. Gray matter connectivity Top row: Population within-eBRS connectivity strength maps in controls, ABST and REL at TP1 (left side) and TP2 (right side). Image left is patient left. Lower rows: Population between-networks connectivity strength maps in controls, ABST and REL at TP1 (left) and TP2 (right). Color bars: Brighter colors or higher numbers indicate ROIs with relatively greater connectivity losses (less connectivity).

60x81mm (300 x 300 DPI)

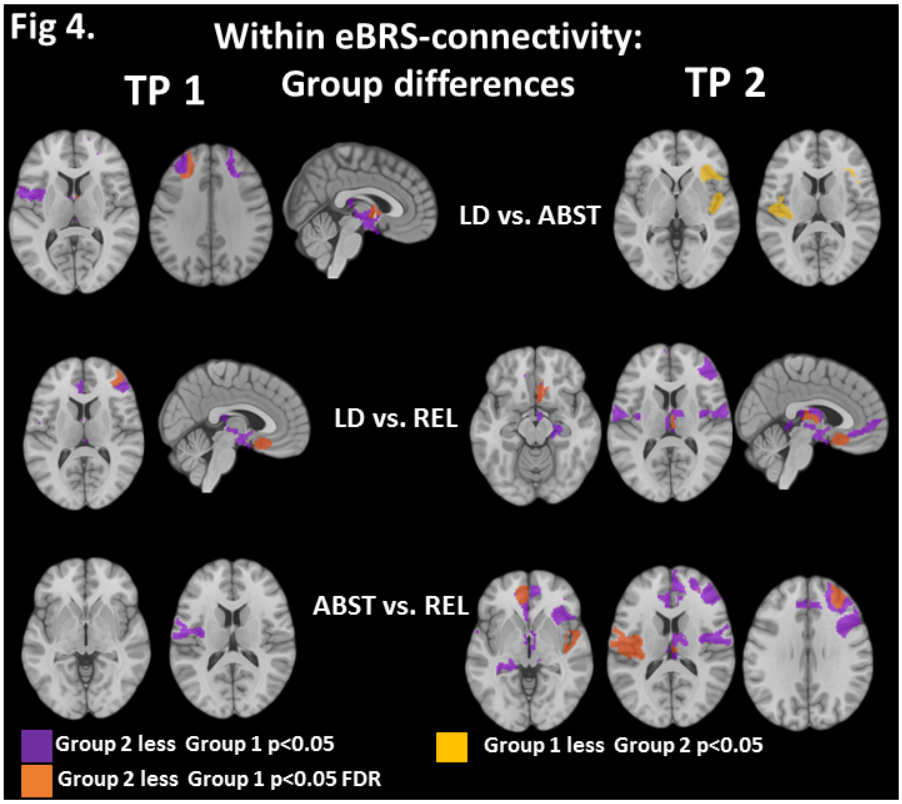

Figure 4. Statistical maps of within-eBRS connectivity. Within-eBRS connectivity differences for different group comparisons at TP1 (left) and TP2 (right). The different colors signify different significance levels ($p<0.05$ with and without FDR correction). Image left is patient left. See text for details.

60x81mm (300 x 300 DPI)

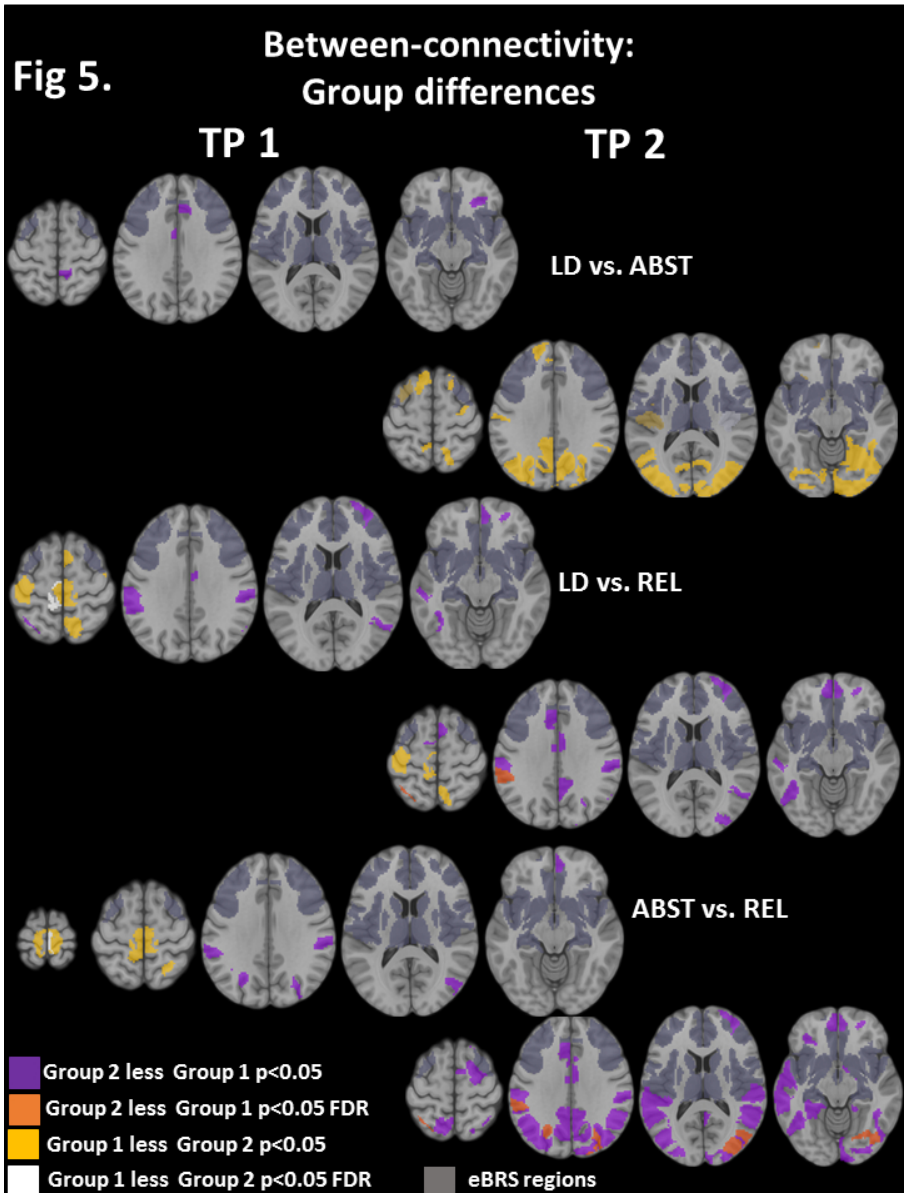

Figure 5. Statistical maps of between-networks connectivity differences at TP (left) and TP2 (right) for different group comparisons. eBRS regions are overlaid in dark gray.
The different colors signify different significance levels (p<0.05 with and without FDR correction). Image left is patient left. See text for details.

60x81mm (300 x 300 DPI)